Concurrent Dual-band Power Amplifier Model Modification using Dual Two-Tone Test

Shoaib Amin*†, Zain Ahmed Khan*†, Magnus Isaksson*, Peter Händel†, and Daniel Rönnow*
* Dept. Electronics, Mathematics, and Natural Sciences, University of Gävle. 80176 Gävle.
† ACCESS Linnaeus Centre, Department of Signal Processing, KTH Royal Institute of Technology, 10044 Stockholm.
Email: shoaib.amin@hig.se

***Abstract*—A dual two-tone technique for the characterization of memory effects in concurrent dual-band transmitters is revisited to modify a 2D-DPD model for the linearization of concurrent dual-band transmitters. By taking into account the individual nonlinear memory effects of the self- and cross-kernels, a new 2D modified digital pre-distortion (2D-MDPD) model is proposed, which not only supersedes the linearization performance but also reduces the computational complexity compared to the 2D-DPD model in terms of number of floating point operations (FLOPs). Experimental results show an improvement of 1.7 dB in normalized mean square error (NMSE) and a 58% reduction in number of FLOPs.**

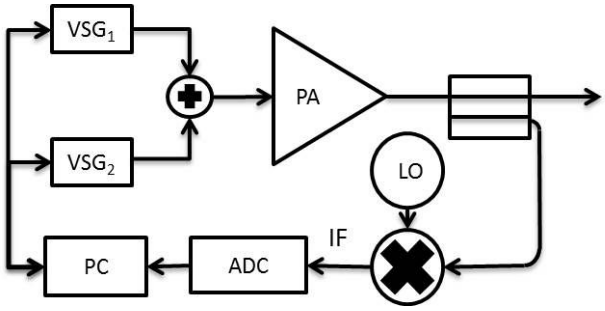

Fig. 1: Measurement setup.

I. Introduction

Digital pre-distortion (DPD) is one of the most cost effective and commonly used techniques for mitigating nonlinear distortions in radio frequency (RF) power amplifiers (PAs). The idea of DPD is to invert the nonlinear transfer function of the PAs such that the cascade of the pre-distorter and PA is a linear function. With the increase in data rates, multi-band multi-standard RF PAs are being considered that can concurrently amplify signals in widely separated bands [1],[2].

When operating PAs with concurrent dual band signals of large frequency separation, single-input single-output (SISO) models are not used; the input signals are generated and up-converted separately and the output signals are received individually. Also, SISO models do not include the effects of cross modulation (CM)[3]. Thus, DPD models that include both IM and CM terms are required [1]. In [3], a 2D-DPD model was proposed for linearization of concurrent dual-band PAs, which is an extension of SISO parallel Hammerstein (PH) model [4]. The major draw-back with the 2D-DPD model is its large number of model coefficient which may lead to numerical instability [1],[2]. In [5] and [6], the 2D modified memory polynomial model and the 2D augmented Hammerstein model were proposed for reducing the model parameters. However, models in [5] and [6] requires combersome identification algorithms which increases the implementation complexity of these models. To alleviate the ill-condition of the 2D-DPD model, an orthogonal 2D-DPD model is proposed in [2], however, the linearization performance is lower than the 2D-DPD model.

An interesting similarity between previously published models is that for self- and cross-kernels, these models use the same memory depth which leads to an increase in computational complexity of the DPD models while implementing in digital platforms. However, studies conducted in [7] contradict with the above assumption. It is shown in [7] that the self-kernels show significantly larger memory effects compared to the cross-kernels. In this paper, we utilize the method proposed in [7] to characterize the individual memory effects of self- and cross-kernels in a concurrent dual-band PA. Based upon the characterization of memory effects, the 2D-DPD model is modified to alleviate its computational complexity. The proposed model is referred to as 2D-modified DPD (2D-MDPD) model.

II. Theory

A. Dual two-tone test

A two-tone technique is a finger print method for characterizing the memory effects of dynamic nonlinear systems [8]. In a two-tone test, frequency dependency and the asymmetry between upper and lower intermodulation (IM) distortion products versus tone spacing are used as a qualitative measures of memory effects. In [7], the technique is extended to characterize the memory effects of a concurrent dual-band transmitters. The technique proposed in [7] gives the possibility to characterize the memory effects that contribute to the asymmetry of upper and lower IM (self-kernels) and CM (cross-kernels) products individually. This in return helps to identify whether the self- and cross-kernels have the same or different memory effects. Moreover, with the dual two-tone test, the similarity between the memory effects appearing at two different carrier frequencies can also be analyzed. Note that, the technique in [7] has not been used for improving the DPD performance of any published models.

In dual two-tone test, each band is excited with a two-tone test signals that are symmetric around their respective carrier frequencies. The test signals are designed according

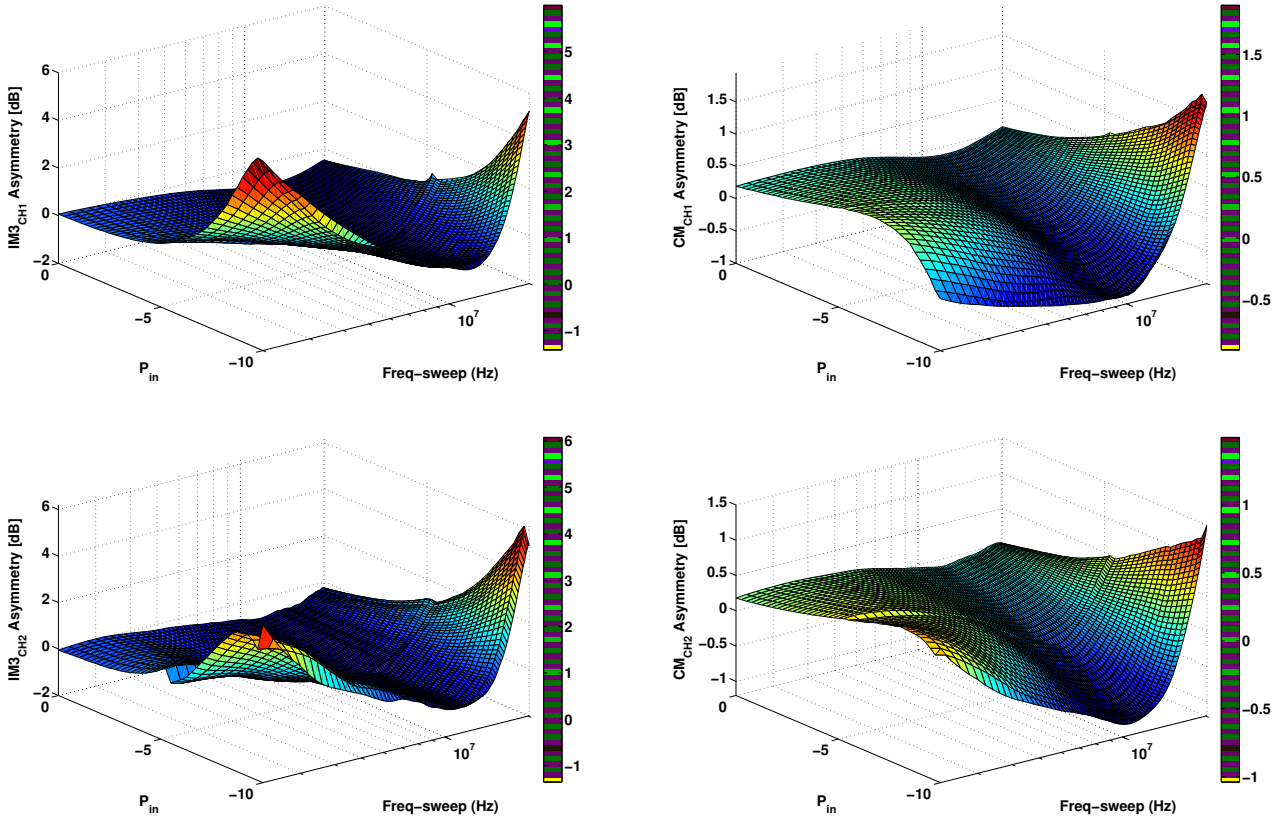

Fig. 2: Asymmetry energy surface of upper and lower intermodulation (IM) (top-left) and cross-modulation (CM) (top-right) products at carrier frequency of 2.0 GHz. Asymmetry energy surface of upper and lower intermodulation (IM) (bottom-left) and cross-modulation (CM) (bottom-right) products at carrier frequency of 2.3 GHz.

to [7] and the tone spacing is defined as, $\Delta\omega_L > \Delta\omega_U$; where $\Delta\omega_L$ is the tone spacing of the signal operating at lower band and $\Delta\omega_U$ is the tone spacing of the signal operating at upper band. The difference in tone space between the two two-tone signals is necessary to distinguish IM and CM distortion products and to avoid overlapping of these products [7]. For the evaluation of asymmetry between different distortion products, 3D energy surfaces are used [7]. 3D energy surfaces have been previously used to study the memory effects that contribute to the asymmetry between upper and lower IM products [9], as a function of frequency spacing and input power levels.

Fig. 2 shows the 3D energy surfaces of the IM and CM products at the carrier frequencies of 2.0 and 2.3 GHz, respectively. From Fig. 2, a noticeable difference between the asymmetric behavior of the IM (top-left) and the CM (top-right) products can be observed at carrier frequency of 2.0 GHz, where the IM products exhibit significant memory effects which contribute to the asymmetry compared to the CM products. A similar observation can be made from Fig. 2, where the IM products (bottom-left) at a carrier frequency of 2.3 GHz also exhibit significant memory effects compared to the CM products (bottom-right).

The analysis yields two important observations; first, the IM products exhibit larger memory effects than the CM products. Second, the IM and CM products at two different carrier frequencies exhibit approximately the same asymmetric behavior, indicating similar memory effects that contribute to the asymmetry at two bands. This information can be utilized for modifying a 2D-DPD model in terms of memory depth. Note that the analysis above is not restricted to concurrent dual-band transmitters and DPD models. This technique could also be used for DPD models of MIMO transmitters.

B. 2D modified DPD model

A 2D-DPD model can be described as [3],

$$y_i(n) = \sum_{m=0}^{M}\sum_{p=0}^{P-1}\sum_{q=0}^{p} h_{mpq}^{(i)} x_i(n-m) \times |x_i(n-m)|^{(p-q)}|x_j(n-m)|^q, \quad \text{where } i \neq j, \tag{1}$$

where $h_{mpq}^{(i)}$ are the model parameters, $x_i(n)$, $x_j(n)$ are the input signals of i^{th} and j^{th} channels, respectively, and $y_i(n)$ is the output of i^{th} channel. M is the memory depth and P is the nonlinear order.

For a third nonlinear order, (1) will contain linear terms $x_i(n-m)$, self-kernels $x_i(n-m)|x_i(n-m)|^2$, and two cross-kernels given as $x_i(n-m)|x_j(n-m)|^2$ and $x_i(n-m)|x_i(n-m)||x_j(n-m)|$, respectively. Notice that, in (1) both the self- and cross-kernels have the same memory depth.

However, from the dual two-tone test, it is observed that the IM (self-kernels) and CM (cross-kernels) products do not exhibit the same memory effects. Thus, by using different memory depth for the IM and CM terms overmodelling can be avoided and the computational cost can be reduced.

In the following, we present a 2D modified DPD model (2D-MDPD), where the modification is being made in terms of memory depth. The 2D-MDPD model can be described as,

$$y_i(n) = \sum_{m_1=0}^{M_1} \sum_{p=1}^{\frac{P+1}{2}} h_s^{(i)} x_i(n-m_1)|x_i(n-m_1)|^{2(p-1)} + \sum_{m_2=0}^{M_2} \sum_{q=2}^{\frac{P+1}{2}} h_{c_1}^{(i)} x_i(n-m_2)|x_j(n-m_2)|^{2(q-1)} + \sum_{m_3=0}^{M_3} \sum_{\substack{p=2 \\ \text{even}}}^{P-1} \sum_{q=1}^{p-1} h_{c_2}^{(i)} x_i(n-m_3)|x_i(n-m_3)|^{(p-q)}|x_j(n-m_3)|^{(q)}, \tag{2}$$

where $h_s^{(i)}$ are the model parameters for self-kernels, $h_{c_1}^{(i)}$ and $h_{c_2}^{(i)}$ are the model parameters for cross-kernels. In (2), M_1, M_2 and M_3 are the respective memory depths of the self- and cross-kernels.

III. Experimental

A. Test setup

The experimental setup is shown in Fig. 1 and is composed of two R&S SMBV100a vector signal generators (VSGs), a wide-band down converter and an ADQ 214 SP devices analog-to-digital converter. The VSGs have baseband and RF coherency. Baseband coherency ensures that the signals from the VSGs are triggered at the same time. The baseband and RF coherency is needed to have full control of the signals at the RF level, required for DPD scheme. The setup was automated with a computer that allows full control over the excitation signals. The device under test (DUT) was a wide-band Mini-Circuits ZVE8G+ power amplifier. Two separate wide-band code division multiple access (WCDMA) signals with peak-to-average-power-ratio (PAPR) of 7.74- and 7.3-dB, respectively, were used to analyze the DPD performance of the models given in (1) and (2). The WCDMA signals, x_1 and x_2, each with 40960 samples were created in the baseband and up-converted to the carrier frequencies of 2.0 and 2.3 GHz, respectively. The combined signal was fed to the DUT.

A similar setup was used for the characterization of memory effects using dual two-tone test signals, where the signals were two two-tone signals with varying tone spacing and input power. During the dual two-tone test, $\Delta\omega_L$ was defined as $2\pi(\Delta_f + \delta_f)$ and $\Delta\omega_U$ was defined as $2\pi(\Delta_f)$, where Δ_f was varying from $2-20$ MHz, whereas, δ_f was constant and had a value of 100 kHz. The input power for the test signals was swept from -10 to 0 dBm with a step size of 0.25 dBm.

B. System identification

The output signal model of a concurrent dual-band PA can be written as

$$\begin{bmatrix} \boldsymbol{y}_1 \\ \boldsymbol{y}_2 \end{bmatrix} = \begin{bmatrix} \boldsymbol{\Phi_1} & 0 \\ 0 & \boldsymbol{\Phi_2} \end{bmatrix} \begin{bmatrix} \boldsymbol{\theta}_1 \\ \boldsymbol{\theta}_2 \end{bmatrix}$$

where $\boldsymbol{y}_i$ is a column vector containing the measured and sampled output signal of i^{th} channel, $\boldsymbol{\theta}_i$ denotes the vector of the model parameters to be estimated, and $\boldsymbol{\Phi}_i = f(x_1, x_2)$ is the regression matrix, whose columns are the basis functions of the 2D-MDPD model. To estimate the pre-distorter, the input and output signals are interchanged in (1) and (2). This is in accordance with indirect learning architecture, where the post-distorter function is the same as pre-distorter [10]. To estimate the model parameters, a least square technique is used.

$$\hat{\boldsymbol{\theta}}_i = (\boldsymbol{\Phi}_i^H \boldsymbol{\Phi}_i)^{-1} \boldsymbol{\Phi}_i^H \boldsymbol{y}_i, \text{where}\, i = \{1, 2\}. \tag{3}$$

The performance of the proposed model was evaluated in terms of normalized mean square error (NMSE) and adjacent channel power ratio (ACPR). The computational complexity of the models is also evaluated in terms of number of complex-valued model coefficients and in number of floating point operations (FLOPs).

IV. Results

The performance of the proposed 2D-MDPD model is compared to the 2D-DPD model. For PA linearization, the nonlinear order and memory depth for (1) was $P = 9$ and $M = 4$ and for 2D-MDPD (2), the nonlinear order was same, and the memory depths were $M_1 = 4$, $M_2 = 2$, and $M_3 = 1$. This choice of nonlinear order and memory depth resulted in the lowest model error.

Table I summarizes the performance comparison of the 2D-DPD and 2D-MDPD models in terms of NMSE and ACPR for channel 1 and 2, respectively. In the absence of any pre-distorter, the measured NMSE was -30.3- and -29.7-dB for channel 1 and 2, respectively; the measured ACPR for channel 1 and 2 was -40.1- and -39.9-dB, respectively. In terms of NMSE, the 2D-DPD model resulted in an NMSE of -42.6 dB for channel 1, whereas, the 2D-MDPD resulted in an NMSE of -44.3 dB, i.e., an improvement of 1.7 dB compared to the 2D-DPD model. Similarly for channel 2, the 2D-MDPD model resulted in an NMSE of -45.1 dB, i.e., a 2.4 dB improvement compared to the 2D-DPD model, which resulted in an NMSE of -42.7 dB. In terms of ACPR, both the 2D-DPD and 2D-MDPD models resulted in approximately the same performance, where the 2D-DPD resulted in slightly higher ACPR by 0.8 dB in channel 1 and 0.3 dB in channel 2 compared to the 2D-MDPD model. In terms of number of complex-valued coefficients, the 2D-DPD model resulted in 180 coefficients per channel, whereas, the 2D-MDPD model resulted in 69 coefficients, i.e., 2.6 times fewer than the 2D-DPD model.

Model complexity in this paper has also been measured based upon the number of FLOPs. Following the methodology in [11], the computational complexity of the models is evaluated as the sum of the total number of FLOPs required in: (a) creation of the basis functions and (b) multiplication of the basis functions with their respective model coefficients referred to as the filtering process. The number of FLOPs required for various arithmetic operations is given in [11]. Therefore, the complexity of creating basis functions in the 2D-DPD model, $C_b^{\text{2D-DPD}}$, can be described as,

$$C_b^{\text{2D-DPD}} = 18 + (P-1)^2. \tag{4}$$

TABLE I: Comparison of the 2D-DPD and 2D-MDPD predistorters

Model	# of FLOPs (# of coefficients)	NMSE CH1 / CH2	ACPR CH1 / CH2
No DPD	–	-30.3 / -29.7 dB	-40.1 / -39.8 dB
2D-DPD	1162 (180)	-42.6 / -42.7 dB	-59.6 / -56.5 dB
2D-MDPD	457 (69)	-44.3 / -45.1 dB	-58.8 / -56.2 dB

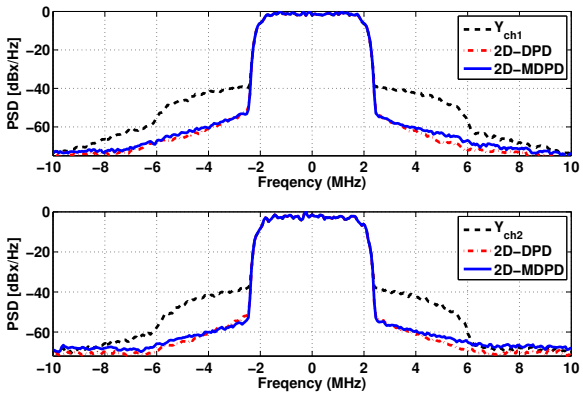

Fig. 3: Measured power spectral density (PSD) vs frequency for DPD.

The filtering process involves complex-valued multiplications of the model parameters $h_{mpq}^{(i)}$ with the corresponding basis functions. Therefore, the filtering complexity, $C_f^{\text{2D-DPD}}$, depends on the number of basis functions and can be described as,

$$C_f^{\text{2D-DPD}} = \frac{6MP\,(P+1)}{2}. \tag{5}$$

The basis functions of the 2D-MDPD exhibits the same structure as the 2D-DPD model but do not include even order terms. Therefore, the complexity of creating basis functions in the 2D-MDPD model, $C_b^{\text{2D-MDPD}}$, can be described as,

$$C_b^{\text{2D-MDPD}} = 18 + \frac{(P+1)^2}{4}. \tag{6}$$

The filtering complexity of the 2D-MDPD model, $C_f^{\text{2D-MDPD}}$ can be described as,

$$C_f^{\text{2D-MDPD}} = 6\left\{(M_1+1)(\frac{P+1}{2})+ \right.$$
$$\left.(M_2+1)(\frac{P+1}{2}-1)+(M_3+1)\left(\sum_{\substack{p=3\\ \text{p odd}}}^{P} p-2\right)\right\} \tag{7}$$

where, $(M_1+1)\frac{P+1}{2}$ are the number of basis functions of the self-kernels and, $(M_2+1)(\frac{P+1}{2}-1)$ and $(M_3+1)\left(\sum_{\substack{p=3\\ \text{p odd}}}^{P} p-2\right)$ are the number of basis function of the cross-kernels. The total number of FLOPs required by 2D-MDPD model are 457, which is approximately 2.5 times less than the 2D-DPD model, which resulted in 1162 FLOPs.

V. Discussion and Conclusion

The continual strive for increasing data rates and use of advance multi-band multi-standards RF transmitter to accommodate multiple signals requires techniques for the characterization of nonlinear dynamic effects of multi-band PAs. These techniques can be utilized to modifying previously published DPD models.

A reference method is used to characterize the individual memory effects of self- and cross-kernels in a dual-band PA. The results show that the memory effects are more dominant in the self-kernels than the cross-kernels. The information extracted from the dual two-tone test resulted in a modification of 2D-DPD model. The proposed 2D-MDPD model not only resulted in an improvement of 1.7- and 2.4-dB in NMSE for channel 1 and 2, respectively, and a comparative performance measured in terms of ACPR; the computation complexity is also reduced by 58 % in terms of number of FLOPS compared to the state of the art 2D-DPD model.

The dual two-tone technique can also be used to characterize MIMO transmitters and for the modification of MIMO DPD model, where the computation complexity is more pronounced than the concurrent dual-band transmitter [7].

References

[1] C. Quindroit, N. Naraharisetti, P. Roblin, S. Gheitanchi, V. Mauer, and M. Fitton, "FPGA Implementation of Orthogonal 2D Digital Predistortion System for Concurrent Dual-Band Power Amplifiers Based on Time-Division Multiplexing," *IEEE Trans. Microw. Theory Techn.*, vol. 61, no. 12, pp. 4591–4599, Dec 2013.

[2] G. Yang, F. Liu, L. Li, H. Wang, C. Zhao, and Z. Wang, "2D orthogonal polynomials for concurrent dual-band digital predistortion," in *IEEE Int. Microw. Symp. Dig.*, Seattle, WA, June 2013, pp. 1–3.

[3] S. Bassam, W. Chen, M. Helaoui, F. Ghannouchi, and Z. Feng, "Linearization of Concurrent Dual-Band Power Amplifier Based on 2D-DPD Technique," *IEEE Trans. Microw. Theory Tech.*, vol. 21, no. 12, pp. 685–687, Dec 2011.

[4] M. Isaksson and D. Wisell, "Extension of the Hammerstein model for power amplifier applications," in *63rd ARFTG Conf. Dig.*, Fort Worth, TX, 2004, pp. 131–137.

[5] Y.-J. Liu, W. Chen, B. Zhou, J. Zhou, and F. Ghannouchi, "2D augmented Hammerstein model for concurrent dual-band power amplifiers," *Electronics Letters*, vol. 48, no. 19, pp. 1214–1216, Sept 2012.

[6] Y.-J. Liu, W. Chen, J. Zhou, B.-H. Zhou, and F. Ghannouchi, "Digital Predistortion for Concurrent Dual-Band Transmitters Using 2-D Modified Memory Polynomials," *IEEE Trans. Microw. Theory Tech.*, vol. 61, no. 1, pp. 281–290, Jan 2013.

[7] S. Amin, W. Van Moer, P. Händel, and D. Rönnow, "Characterization of Concurrent Dual-Band Power Amplifiers Using a Dual Two-Tone Excitation Signal," *IEEE Trans. Instrum. Meas.*, vol. 64, no. 10, pp. 2781–2791, Oct 2015.

[8] D. Wisell, B. Rudlund, and D. Rönnow, "Characterization of Memory Effects in Power Amplifiers Using Digital Two-Tone Measurements," *IEEE Trans. Instrum. Meas.*, vol. 56, no. 6, pp. 2757–2766, Dec 2007.

[9] J. Kenney and P. Fedorenko, "Identification of RF Power Amplifier Memory Effect Origins using Third-Order Intermodulation Distortion Amplitude and Phase Asymmetry," in *IEEE Int. Microw. Symp. Dig.*, San Francisco, CA, June 2006, pp. 1121–1124.

[10] C. Eun and E. Powers, "A new Volterra predistorter based on the indirect learning architecture," *IEEE Trans. Signal Process.*, vol. 45, no. 1, pp. 223–227, Jan 1997.

[11] A. Tehrani, H. Cao, S. Afsardoost, T. Eriksson, M. Isaksson, and C. Fager, "A comparative analysis of the complexity/accuracy tradeoff in power amplifier behavioral models," *IEEE Trans. Microw. Theory Techn.*, vol. 58, no. 6, pp. 1510–1520, Jun. 2010.